# Reduced classical trajectory equations for electronically non-adiabatic transition on photochemical pericyclic reactions

**Kenji Morihashi and Osamu Kikuchi**

Department of Chemistry, The University of Tsukuba, Sakura, Ibaraki 305, Japan

It may be difficult to use the classical trajectory equations (CTE) for the estimation of electronically non-adiabatic transition probabilities in photochemical pericyclic reactions because of many nuclear degrees of freedom. In order to avoid this difficulty, the CTE were reformulated in terms of the reaction path coordinates, and the reduced CTE were derived, in which the system was restricted to move one-dimensionally along the postulated reaction path. As an application, the non-adiabatic decay from the lowest excited state to the ground state was investigated for the conrotatory and disrotatory processes of the photochemical electrocyclic reaction of 1,3-cis-butadiene to form cyclobutene.

**Key words:** Photochemical pericyclic reactions—non-adiabatic transition—classical trajectory equations—butadiene—cyclobutene

## 1. Introduction

In organic photochemical reactions, there are several types of avoided surface crossings [1]. The electronically non-adiabatic transition in such an avoided crossing region often plays an important role in photochemical phenomena [1-3]. In this paper, we will consider the significant non-adiabatic transition involved in photochemical pericyclic reactions [4].

The non-adiabatic transition in photochemical pericyclic reactions may be described properly by the classical trajectory approach [5]. The classical trajectory equations (CTE) are written in terms of adiabatic state functions $\{\Psi_\alpha(t)\}$ and

the energies $\{E_\alpha(t)\}$ as:

$$\dot{a}_\alpha = -\sum_{\beta \neq \alpha} \langle \Psi_\alpha | \partial/\partial t | \Psi_\beta \rangle \exp\left[-(i/\hbar) \int^t (E_\beta - E_\alpha)\, dt\right] a_\beta. \tag{1}$$

Since $\Psi_\alpha(t)$ depends on the time through the nuclear trajectory $R(t)$ which is usually represented by the internal nuclear coordinates $\{q_j(t)\}$ of the $N$-atom system, the coupled equations (1) become as follows:

$$\dot{a}_\alpha = -\sum_{\beta \neq \alpha} \sum_j^{3N-6} \langle \Psi_\alpha | \partial/\partial q_j | \Psi_\beta \rangle \dot{q}_j \exp\left[-(i/\hbar) \int^t (E_\beta - E_\alpha)\, dt\right] a_\beta. \tag{2}$$

Recently, the systematic treatments based on Eqs. (2) have been applied to some unimolecular reaction systems by Lorquet and his coworkers [6-9]. The non-adiabatic coupling terms, $\langle \Psi_\alpha | \partial/\partial q_j | \Psi_\beta \rangle$, are important to obtain the transition probability between states, $\Psi_\alpha$ and $\Psi_\beta$, and have been calculated by several authors [10-12]. Many non-adiabatic coupling terms in Eq. (2), however, make the CTE treatment very difficult, since the evaluation of coupling term is very laborious.

Our present intention is not to discuss the rigorous solutions of Eq. (2) but to obtain the approximate solutions with a qualitative accuracy enough to determine the most probable path among several postulated ones. In order to obtain such solutions in a simple way, the flexibility of nuclear motion of the polyatomic system needs to be restricted according to the characteristics of pericyclic reactions.

The pericyclic reactions can be well described with a molecular orbital (MO) correlation diagram [4]. During the photochemically-allowed processes in the Woodward–Hoffmann rule [4], a crossing occurs between the highest occupied MO(HOMO) and the lowest unoccupied MO(LUMO). Such a crossing indicates the drastic change in the electronic configurations of the ground state and the excited state; both states usually have the same spin and spatial symmetry properties. Thus the two states interact non-adiabatically due to the specific motion along the symmetry-preserved reaction path. Therefore, the non-adiabatic coupling term for the reaction coordinate is regarded as a dominant factor of the non-radiative decay between the states. This is a key to treat Eq. (2) in a simple way for organic reaction systems. In spite of the complexity due to many nuclear degrees of freedom, CTE may be reduced to the one-dimensional problem for the reaction coordinate.

In the next section, an alternative form of CTE will be derived in terms of the reaction path coordinates [13] instead of the internal nuclear coordinates $\{q_j\}$. The non-adiabatic coupling terms will be resolved into that due to the motion along the reaction path and those due to the motions fluctuating from the reaction path. In Sect. 3, the alternative CTE will be reduced to the one-dimensional problem for the reaction coordinate by neglecting the coupling terms due to the fluctuating motions. The significant coupling term can be evaluated by means of a finite difference of the reaction coordinate, which can be defined as the

mass-weighted distance of the reaction path [13–16]. The Landau–Zener model [17–19] is employed to obtain the approximate solution of the reduced CTE. This method will be applied in Sect. 4 to the photochemical electrocyclic reaction of butadiene to compare the non-adiabatic transitions between the stereochemically different paths.

## 2. An alternative form of CTE

Instead of the internal nuclear coordinates $\{q_j\}$, the mass-weighted Cartesian coordinates are adopted,

$$\boldsymbol{a}_i = (a_{ix}, a_{iy}, a_{iz}) = (\sqrt{m_i}\,r_{ix}, \sqrt{m_i}\,r_{iy}, \sqrt{m_i}\,r_{iz}), \; i = 1, 2, \ldots, N, \tag{3}$$

where $r_i$ is the position vector for atom $i$ and $m_i$ is the mass. The nuclear position on a specific reaction path is described with a time-dependent vector in the mass-weighted Cartesian coordinate space:

$$\boldsymbol{A}(t) = \{\boldsymbol{a}_i\} = \{\boldsymbol{a}_1, \boldsymbol{a}_2, \ldots, \boldsymbol{a}_N\}. \tag{4}$$

Hereafter the following notations are used for all vectors; a three-dimensional vector is represented with a boldfaced small letter, e.g., $\boldsymbol{v}_i = (v_{ix}, v_{iy}, v_{iz})$ for atom $i$, and a $3N$-dimensional vector is represented with a boldfaced capital letter, e.g., $\boldsymbol{V} = (\boldsymbol{v}_1, \boldsymbol{v}_2, \ldots, \boldsymbol{v}_N)$.

The reaction coordinate is defined as the mass-weighted distance along the reaction path [13–16]:

$$s(t) = \int_A ds, \tag{5}$$

and

$$ds(t_0) = \lim_{t_1 \to t_0} |\boldsymbol{A}(t_1) - \boldsymbol{A}(t_0)| = \lim_{t_1 \to t_0} \sum_i |\boldsymbol{a}_i(t_1) - \boldsymbol{a}_i(t_0)|$$

$$= \left( \sum_i |d\boldsymbol{a}_i/dt_0|^2 \right)^{1/2} dt_0. \tag{6}$$

Therefore, the reaction path $\boldsymbol{A}(t)$ is dependent on time $t$ through the reaction coordinate $s(t)$, i.e., $\boldsymbol{A}(s(t)) = \{\boldsymbol{a}_i(s)\}$. It should be noted that the nuclear geometry of a reaction system is determined by only one variable, $s$, if the reaction path is specified. In this case, $\boldsymbol{A}(t)$ is equivalent to the nuclear trajectory $\boldsymbol{R}(t)$ which consists of one-dimensional motion along the reaction path only.

In order to consider a more flexible trajectory, let $\boldsymbol{R}(t)$ involve not only the motion along the reaction path but also the fluctuating motions which are orthogonal to the reaction path, i.e.,

$$\boldsymbol{R}(t) = \boldsymbol{A}(s) + \boldsymbol{D}(s), \tag{7}$$

where $\boldsymbol{D} = \{\boldsymbol{d}_i\}$, $i = 1, 2, \ldots, N$, is the displacement vector from the reaction path $\boldsymbol{A}(s)$, which is assumed to be orthogonal to the unit vector $(d\boldsymbol{A}/ds)$ directed to

the reaction path:

$$\mathbf{D} \cdot (d\mathbf{A}/ds) = \sum_i \mathbf{d}_i \cdot (d\mathbf{a}_i/ds) = 0. \tag{8}$$

If $3N-7$ orthonormalized vectors $\mathbf{U}_k = \{\mathbf{u}_{ik}\}$, $i = 1, 2, \ldots, N$, perpendicular to the reaction path, are introduced formally,

$$\mathbf{U}_k \cdot \mathbf{U}_l = \sum_i \mathbf{u}_{ik} \cdot \mathbf{u}_{il} = \delta_{kl}, \quad k, l = 1, 2, \ldots, 3N-7, \tag{9}$$

$$\mathbf{U}_k \cdot (d\mathbf{A}/ds) = \sum_i \mathbf{u}_{ik}(d\mathbf{a}_i/ds) = 0, \quad \text{for all } k, \tag{10}$$

the nuclear trajectory $\mathbf{R}(t)$ can be written by

$$\mathbf{R}(t) = \mathbf{A}(s) + \sum_{k=1}^{3N-7} Q_k(s)\mathbf{U}_k, \tag{11}$$

where the coefficients $Q_k$ are given by

$$Q_k(s) = \sum_i \mathbf{d}_i(s) \cdot \mathbf{u}_{ik}. \tag{12}$$

The variables, $s, \{Q_k\}, k = 1, 2, \ldots, 3N-7$, are called the reaction path coordinates [13]. Consequently, the time differential operator in Eq. (1) can be replaced by

$$\partial/\partial t = (\partial/\partial s)\dot{s} + \sum_k^{3N-7} (\partial/\partial Q_k)\dot{Q}_k \tag{13}$$

Inserting Eq. (13) into Eq. (1), the alternative form of CTE is obtained in terms of the rection path coordinates:

$$\dot{a}_\alpha = -\sum_{\alpha \neq \beta} \{g_{\alpha\beta}^{(s)}\dot{s} + \sum_k g_{\alpha\beta}^{(k)}\dot{Q}_k\} \exp\left[-(i/\hbar)\int^t (E_\beta - E_\alpha)\,dt\right] a_\beta, \tag{14}$$

where

$$g_{\alpha\beta}^{(s)} = \langle\Psi_\alpha|\partial/\partial s|\Psi_\beta\rangle, \tag{15}$$

$$g_{\alpha\beta}^{(k)} = \langle\Psi_\alpha|\partial/\partial Q_k|\Psi_\beta\rangle, \quad k = 1, 2, \ldots, 3N-7. \tag{16}$$

The coupling terms $g_{\alpha\beta}^{(s)}$ and $g_{\alpha\beta}^{(k)}$ express the non-adiabatic interaction between the $\alpha$ and $\beta$ states due to the motion along the reaction path and due to the fluctuating motions orthogonal to the reaction path, respectively.

## 3. Method of reduced CTE

In photochemically-allowed processes of pericyclic reactions, the two lowest singlet states interact non-adiabatically along a symmetry-preeserved reaction path. This can be understood from the MO or state correlation diagram [4, 20, 21]. For example, in the butadiene-cyclobutene system which is discussed in the later section, a crossing between HOMO and LUMO is involved in the MO correlation diagram (Fig. 1a) for the disrotatory process. As may be seen from the state correlation diagram (Fig. 1b), the MO crossing corresponds to the
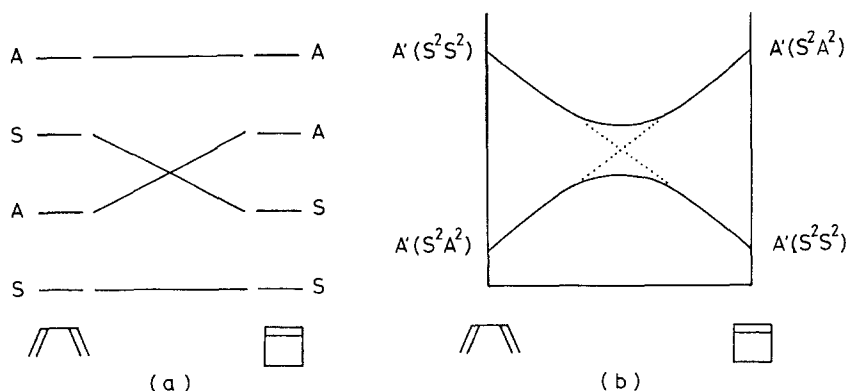
**Fig. 1a.** The MO correlation diagram for the disrotatory mode of the butadiene-cyclobutene system. The molecular orbitals are labelled as $S$ (for symmetric) or $A$ (for antisymmetric) with respect to a symmetry plane which is preserved throughout the reaction. **b** The state correlation diagram. The main electronic configurations of the two symmetric singlet states are shown in ( )

exchange of the main electronic configuration, $(S^2S^2)$ or $(S^2A^2)$, between the ground and lowest excited states. This is a common factor in the photochemically-allowed processes of pericyclic reactions. Thus the electronic state functions are forced to change the components drastically by the motion along the reaction path, while the fluctuating motions orthogonal to the reaction path may give only the secondary effects to the non-adiabatic transition between the states. In other words, the coupling terms $g_{\alpha\beta}^{(k)}$ due to the fluctuating motions may be negligibly small in comparison with the reaction coordinate coupling term $g_{\alpha\beta}^{(s)}$ in the avoided crossing region.

Then we assume that the coupling term $g_{\alpha\beta}^{(k)}$ for all $Q_k$ can be neglected in Eq. (14). If only two adiabatic states $(\alpha, \beta = 1, 2)$ are taken into account, Eq. (14) become under the assumption as follows:

$$
\dot{a}_1 = +g\dot{s} \exp\left[ -(i/\hbar) \int^t \Delta E \, dt \right] a_2,
$$

$$
\dot{a}_2 = -g\dot{s} \exp\left[ +(i/\hbar) \int^t \Delta E \, dt \right] a_1,
$$

$$(17)$$

where

$$
g = \langle \Psi_2 | \partial/\partial s | \Psi_1 \rangle, \quad \Delta E = E_2 - E_1 > 0.
$$

Since Eqs. (17) involve only one nuclear degree of freedom for the reaction coordinate, those have the same form as the CTE of the diatomic molecular system. Hereafter we call Eqs. (17) the reduced CTE.

In calculations of the non-adiabatic coupling term in Eqs. (17), the two adiabatic states are expanded in the spin-symmetry adapted configurations $\{\psi_m\}$:

$$
\Psi_1 = \sum_m A_m \psi_m, \quad \Psi_2 = \sum_m B_m \psi_m.
$$

The non-adiabatic coupling term along the reaction path can be written as a sum of the CI term and the MO term:

$$g = \langle \Psi_2 | \partial / \partial s | \Psi_1 \rangle = g_{CI} + g_{MO}, \tag{18}$$

and

$$g_{CI} = \sum_m B_m (\partial A_m / \partial s), \tag{19}$$

$$g_{MO} = \sum_m \sum_n B_m A_n \langle \psi_m | \partial / \partial s | \psi_n \rangle. \tag{20}$$
$$\begin{subarray}{c} m \; n \\ (m \neq n) \end{subarray}$$

These terms can be evaluated approximately by the method of a finite difference for reaction coordinate. The computational details are given in the previous works [7, 22].

According to Eqs. (17), the transition probability $P_{2 \to 1} = |a_1|^2$ from the $\Psi_2$ state to the $\Psi_1$ state depends on three factors: the non-adiabatic coupling term $g$, the velocity $\dot{s}$ directing to the reaction path and the energy gap $\Delta E$ between $\Psi_1$ and $\Psi_2$. Although the solutions of Eqs. (17) are obtained exactly from the numerical analysis, the approximate solutions based on the Landau–Zener model [17-19] are enough for our present purpose. The method employed here is essentially the same as that demonstrated by Desouter-Lecomte et al. [8, 9].

It is convenient to introduce the diabatic functions $\eta_1$ and $\eta_2$, which obey the condition:

$$\langle \eta_1 | \partial / \partial s | \eta_2 \rangle = 0. \tag{21}$$

The diabatic functions $\{\eta\}$ can be obtained by the unitary transformation of the adiabatic state functions $\{\Psi\}$:

$$\begin{pmatrix} \eta_1 \\ \eta_2 \end{pmatrix} = \begin{pmatrix} \cos \theta & -\sin \theta \\ \sin \theta & \cos \theta \end{pmatrix} \begin{pmatrix} \Psi_1 \\ \Psi_2 \end{pmatrix}. \tag{21}$$

From the condition (21), the mixing angle $\theta$ is written by

$$\theta(s) = \int^s g(s') \, ds'. \tag{22}$$

Since the diabatic states $\{\eta\}$ and the adiabatic states $\{\Psi\}$ must coincide at the initial and final stages of the reaction, the integration of $g$ over the whole coupling region should give the value of $\pi/2$, while $\theta(s_c) = \pi/4$ for the point $s_c$ where two diabatic states intersect. If the variation of $g$ has the Lorenzian shape, the diabatic crossing point $s_c$ corresponds to the point where the $g$ value becomes maximum. Once $s_c$ is determined thus, then the Massey parameter $\xi$ is caluclated by [6-9]

$$\xi = \Delta E(s_c) / \hbar \dot{s}_c g(s_c). \tag{23}$$

The velocity $\dot{s}_c$ is obtained from the kinetic energy $T_s$ along the reaction path. If we give an appropriate value for $T_s$ from the calculated potential energy curves,

the velocity $\dot{s}_c$ at the crossing point can be estimated by $\dot{s}_c = (2T_s)^{1/2}$. By employing the Landau–Zener model [8], the transition probability is calculated by

$$P = \exp\left[-(\pi/4)\xi\right]. \tag{24}$$

In the pericyclic reactions, the energy gap $\Delta E$ becomes so large in comparison with the kinetic energy $T_s$ that the quantum effect of the nuclear motion cannot be neglected in the quantitative prediction for the non-adiabatic transition probability. As pointed out in the previous works [5, 19], such quantum effects are not involved in the classical trajectory scheme. In order to keep the accuracy of CTE for such systems, a large kinetic energy $T_s$ must be given although the value is often unrealistic. The value of $T_s$ employed here is given so as to satisfy the following rough criterion for the classical behavior of nuclear motion:

$$\Delta E(s_c)/T_s(s_c) \ll 1. \tag{26}$$

## 4. Application of the reduced CTE

The method presented in Sect. 3 has been applied to the photochemical electrocyclic reaction of 1,3-cis-butadiene [23–25]. In the isomerization process between substituted 1,3-cis-butadiene and cyclobutene derivatives, there exist two stereochemically different modes of methylene rotations, the conrotatory and disrotatory modes. Of these two modes, only the disrotatory process has been
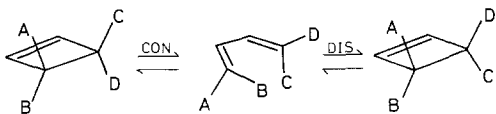


experimentally observed in the photochemical reaction; this is a typical example which can be understood on the basis of the Woodward–Hoffmann rule [4]. The orbital symmetry arguments, however, cannot explicitly answer the question how the excited butadiene decays to the ground state of cyclobutene. In order to describe the dynamics more clearly, the non-adiabatic transition from the lowest excited singlet state to the ground state should be investigated for each reaction mode.

The geometries of cis-butadiene and cyclobutene were optimized by *ab initio* SCF calculations with STO-3G basis set [26]. They are shown in Fig. 2. The linear reaction paths [23] were assumed for the conrotatory and disrotatory modes. The geometries on the reaction pathway from the reactant (butadiene) to the photo-product (cyclobutene) were determined by the linear-path relations of the internal nuclear coordinates $\{q_j\}$:

$$q_j(\tau) = (q_j^P - q_j^R)\tau + q_j^R, \; j = 1, 2, \ldots, 3N - 6, \tag{27}$$

and

$$\tau = s(t)/s_{\text{total}}, \; 0 \le \tau \le 1,$$
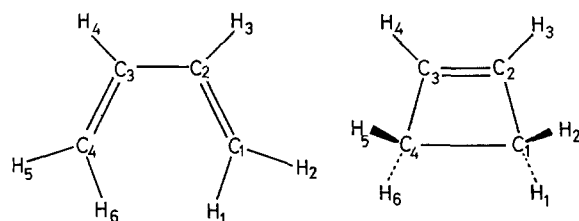
|                    | cis-butadiene | cyclobutene |
| ------------------ | ------------- | ----------- |
| $r(C_1-C_2)$       | 1.314         | 1.526       |
| $r(C_2-C_3)$       | 1.494         | 1.314       |
| $r(C_1-H_1)$       | 1.080         | 1.089       |
| $r(C_1-H_2)$       | 1.080         | 1.089       |
| $r(C_2-H_3)$       | 1.085         | 1.082       |
| $a(C_1C_2C_3)$     | 126.2         | 94.7        |
| $a(H_3C_2C_3)$     | 114.5         | 134.2       |
| $a(H_1C_1C_2)$     | 122.7         | 125.5       |
| $a(H_2C_1C_2)$     | 121.6         | 125.5       |
| $a(H_{12}C_1C_2)$  | 180.0         | 138.4       |

**Fig. 2.** Molecular structures of cis-butadiene and cyclobutene optimized by the STO-3G SCF calculations. Bond lengths, $r(\ )$, in Å, and bond angles, $a(\ )$, are in degrees. The optimized structure of cyclobutene is from Ref. [27]

where $s_{total}$ is the total mass-weighted distance from the reactant to the photoproduct, and $q_j^R$ and $q_j^P$ are the $j$'th internal coordinate of reactant and of photoproduct, respectively. The geometry at each point on the linear reaction path was determined according to Eq. (27) so that the system preserved a twofold symmetry axis in the conrotatory mode and a symmetry plane in the disrotatory mode.

The internal coordinates were transformed into the mass-weighted Cartesian coordinates so that the center of mass is always fixed at the origin and the external translation and the external rotations are excluded from the mass-weighted Cartesian coordinate system. The reaction coordinate was obtained by the numerical integration of Eq. (5) along the reaction path. The total distance from butadiene to cyclobutene is the same for the conrotatory and disrotatory paths; $s_{total} = 9.84$ in unit of $(amu)^{1/2}(bohr)$.

*Ab initio* SCF CI calculations were performed to obtain the potential energy curves according to the manner of Grimbert et al. [25]. The employed AO basis set is the STO-3G plus the diffuse Gaussian $p$ orbitals with an exponent of 0.04 (three degenerate $x$, $y$, and $z$ components were included on each carbon atom). The molecular orbitals were obtained by means of the closed-shell SCF method. For the CI calculation, twelve MO were selected from the $\pi$-MO of butadiene or cyclobutene and from the $\sigma$-MO contributing to the $\pi$-electronic system. From singly- and doubly-excited configurations, 183 configurations were employed for the symmetric singlet states, and 172 configurations for the antisymmetric singlet states. The potential curves obtained thus are shown in Fig. 3, where the lowest symmetric singlet $S_0$ and $S_2$ states and the lowest antisymmetric singlet $S_1$ state
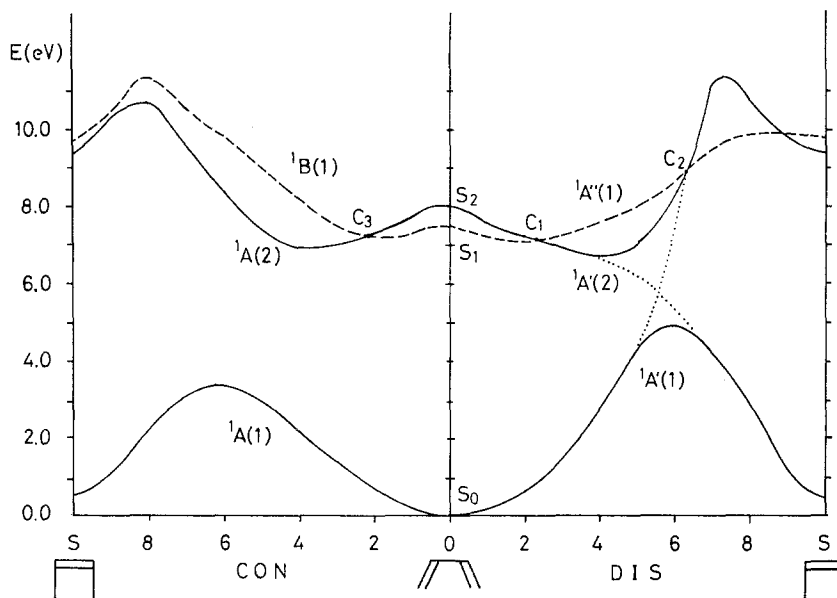
**Fig. 3.** Potential energy curves for the disrotatory and conrotatory modes in the butadiene-cyclobutene system. The $C_s$ symmetry is preserved in the disrotatory process and the $C_2$ symmetry is preserved in the conrotatory process. *Full line*: the lowest symmetric singlet $S_0$ and $S_2$ states. *Dashed line*: the lowest antisymmetric singlet $S_1$ state. Unit of reaction coordinate is $(amu)^{1/2}(bohr)$

are drawn for each reaction mode. In the disrotatory mode, the energy level of $^1A''$ state of the present calculations is slightly higher than that of the previous work [25] because the open-shell SCF MO were not employed in our CI calculations.

Our hypothetical mechanism of the photochemical cyclization of butadiene is explained from the potential energy curves shown in Fig. 3. The reaction is assumed to start from the lowest excited singlet $S_1$ state of butadiene; the internal conversion from the $S_1$ state to the ground state is not discussed in this study. At the early stage of the disrotatory cyclization process, butadiene changes its electronic state from the $^1A''(1)$ state to the $^1A'(2)$ one through the symmetrically-allowed $C_1$ crossing. At the middle stage of the cyclization, the system decays from the $^1A'(2)$ state to the $^1A'(1)$ state from which the ground state of cyclobutene is formed. This mechanism has been first proposed by van der Lugt and Oosterhoff [23], and has been discussed in detail by Grimbert et al. [25]. For the conrotatory cyclization, the mechanism similar to that of the disrotatory one is considered; the reaction starts from the $S_1$ excited state of butadiene, and the ground state of cyclobutene is formed via the non-adiabatic transition from the $^1A(2)$ state to the $^1A(1)$ one.

The potential energy curves in Fig. 3 indicate that the butadiene in its excited $S_1$ state may reach either the $C_1$ or $C_3$ crossing point with nearly equal probability, since, in the early stage of cyclization, there are no potential energy barriers to

the disrotatory and conrotatory rotations of the $S_1$ state of butadiene. In the present hypothetical mechanism, the non-adiabatic transition, $^1A'(2) \rightarrow {}^1A'(1)$ for the disrotatory mode and $^1A(2) \rightarrow {}^1A(1)$ for the conrotatory mode, may play a significant role to determine the stereochemical reaction mode. It is thus necessary to evaluate the non-adiabatic coupling terms between the $S_2$ and $S_0$ states in each reaction mode and to compare the transition probabilities between the conrotatory and disrotatory modes.

The non-adiabatic coupling terms (18) between the two symmetric states were evaluated along each reaction path by using the CI wavefunction obtained above. The numerical accuracy of the coupling term (18) was estimated by the following test [7]:

$$\langle \Psi_2 | \partial/\partial s | \Psi_1 \rangle = -\langle \Psi_1 | \partial/\partial s | \Psi_2 \rangle. \tag{28}$$

The satisfactory results with an accuracy of four significant figures were obtained when the finite difference $\delta s = 0.002$ was used; this corresponds to a simultaneous variation of the internal coordinates (e.g., 0.018 degree of the methylene rotation, $3.8 \times 10^{-5}$ Å variation of the $C_1 - C_2$ bond length, and so on). The calculated $g$ terms are shown in Fig. 4. In the conrotatory mode, the MO term is larger than the CI term (Fig. 4a) and the $g$ shape is broad over the reaction path, where the maximum height is 0.28 at $s = 5.5$. In the disrotatory mode, the CI term is dominant
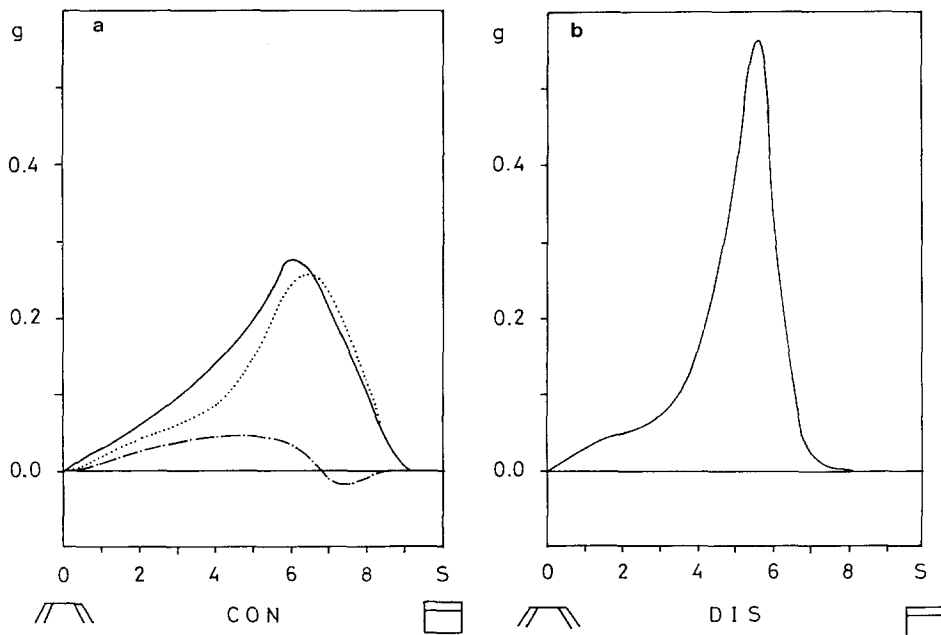


**Fig. 4.** Calculated non-adiabatic coupling term between $^1A(2)$ and $^1A(1)$ states for the conrotatory mode ($a$), and that between $^1A'(2)$ and $^1A'(1)$ states for the disrotatory mode ($b$). Dashed and dotted line: CI term $g_{CI}$; dotted line: MO term $g_{MO}$; full line: the sum $g = g_{CI} + g_{MO}$. Unit of $g$ is $(amu)^{-1/2}(bohr)^{-1}$. In Fig. 4b only the sum is shown, since the MO term is negligibly small

**Table 1.** Transition probabilities and their related quantities for the disrotatory and conrotatory modes of the butadiene-cyclobutene system

|  | $T_s$ (eV) | $\Delta E$ (eV) | $g_{max}$ [a] | $\xi$ | $P_{2\rightarrow 1}$ [b] |
|---|---|---|---|---|---|
| disrotatory | 5.00 | 2.56 | 0.565 | 11.7 | $1.0\times 10^{-4}$ |
| conrotatory | 5.00 | 4.96 | 0.279 | 46.0 | $\simeq 10^{-16}$ |

[a] $g_{max}$ indicates the maximum value of the coupling term in the unit of $(amu)^{-1/2}(bohr)^{-1}$.
[b] The Landau–Zener model was employed in the calculation of transition probability (24)

while the MO term is negligibly small. The $g$ variation is very sharp near the avoided crossing region (Fig. 4b), where the maximum height is 0.56 at $s = 5.9$. Thus the calculated $g$ term shows clearly the difference between the non-adiabatic interaction of the two reaction processes.

The transition probabilities were evaluated and compared between the conrotatory and disrotatory modes. The maximum value of the coupling term $g(s_c)$ and the energy gap $\Delta E(s_c)$, in the Massey parameter (23), were already obtained in above calculations. The kinetic energy $T_s$ at the $s_c$ crossing point was assumed to be 5.0 (eV) for both reaction modes. From the Massey parameter thus obtained, the transition probability for each reaction mode was calculated by Eq. (24). The results are summarized in Table 1. It was found that the transition probability in the disrotatory mode is $10^{12}$ times larger than that in the conrotatory mode. This remarkable difference between the two transition probabilities is considered to be a main reason for the stereospecificity expected in the photochemical electrocyclization of butadiene to cyclobutene.

This interpretation of the stereospecificity in the butadiene-cyclobutene system may be slightly different from the usual arguments with the state correlation diagram [20]. In the qualitative prediction with the state correlation diagram, the conrotatory mode is considered to be disadvantageous for the photochemical cyclization of the butadiene to cyclobutene because of the existence of the energy barrier on the lowest excited $^1B(1)$ state. Although this barrier is observed in the $^1B(1)$ state of the present potential energy curves (Fig. 3), the barrier exists near the cyclobutene side. Hence, the barrier appeared in the $^1B(1)$ state is not an important factor to determine the stereochemical course of the photochemical cyclization reaction of butadiene to cyclobutene.

The decay processes from the excited state of butadiene cannot be well-understood without the multi-dimensional potential energy surfaces of the ground and excited states. Fig. 3 is the one-dimensional cross section of the multi-dimensional surfaces and the energy minima appeared in the $^1A(2)$ and $^1A'(2)$ curves may not be the absolute minima on the multi-dimensional surfaces. If the non-adiabatic transition from these minima to the ground state energy surface is inefficient, the system at the $^1A(2)$ or $^1A'(2)$ minimum region may undergo the structural change which

is not related to the cyclobutene formation. This is expected to occur in the conrotatory process, since the $^1A(2) \to {}^1A(1)$ non-adiabatic transition was calculated to be inefficient. From this point of view, the evaluation of the non-adiabatic coupling between electronic states is important to compare the efficiencies of the postulated processes in photochemical reactions.

In the case of the photochemical ring opening reaction of cyclobutene to butadiene, however, the energy barrier of the antisymmetric state plays a significant role for the stereospecificity. As may be seen from Fig. 3, there is a high energy barrier on the $^1B(1)$ state for the conrotatory ring opening process of cyclobutene, while such a high energy barrier is not found on the $^1A''(1)$ state for the disrotatory mode. This consideration is parallel to the qualitative prediction from the state correlation diagram.

## 5. Conclusion

In the CTE written in terms of the reaction path coordinates, there appear two different types of the non-adiabatic coupling. i.e., the reaction coordinate coupling and the fluctuating coupling. Under the assumption that the nuclear motion along the symmetry-preserved path is most important to induce the non-adiabatic transition from the lowest excited singlet state to the ground state in the photochemical pericyclic reaction system, the reduced CTE have been derived, which involve only the reaction coordinate coupling. Based on this reduced CTE, the transition probability can be obtained simply from the calculated coupling term, energy gap, and velocity. The application to the butadiene-cyclobutene system has shown the usefulness of the reduced CTE. It is expected that, for many photochemical pericyclic reactions, the reduced classical trajectory method is useful to estimate the probability of non-adiabatic transitions involved in some hypothetical reaction paths.

## References

1. Salem, L., Leforestier, C., Segal, G., Wetmore, R.: J. Am. Chem. Soc. 97, 479 (1975)
2. Dauben, W. G., Salem, L., Turro, N.: Accounts. Chem. Res. 8, 41 (1975)
3. Turro, N. J.: Modern Molecular Photochemistry. Menlo Park: Benjamin/Cummings 1978
4. Woodward, R. B., Hoffmann, R.: The Conservation of Orbital Symmetry. New York: Academic Press 1970
5. Tully, J. C., in: Dynamics of Molecular Collisions Part B, Miller, W. H., Ed. New York: Plenum Press 1976
6. Desouter-Lecomte, M., Lorquet, J. C.: J. Chem. Phys. 66, 4006 (1977)
7. Galloy, C., Lorquet, J. C.: J. Chem. Phys. 67, 4672 (1977)
8. Desouter-Lecomte, M., Lorquet, J. C.: J. Chem. Phys. 71, 4391 (1979)
9. Desouter-Lecomte, M., Galloy, C., Lorquet, J. C., Vaz Pires, M.: J. Chem. Phys. 71, 3661 (1979)
10. Hirsch, G., Bruna, P. J., Buenker, R. J., Peyerimhoff, S. D.: Chem. Phys. 45, 335 (1980)
11. Persico, M.: J. Am. Chem. Soc. 102, 7839 (1980)
12. Persico, M., Bonačić-Koutecky, V.: J. Chem. Phys. 76, 6018 (1982)
13. Miller, W. H., Handy, N. C., Adam, J. E.: J. Chem. Phys. 72, 99 (1980)
14. Tachibana, A., Fukui, K.: Theoret. Chim. Acat. (Berl.) 49, 321 (1978)
15. Mezey, P. G.: Theoret. Chim. Acta. (Berl.) 54, 95 (1980)

16. Fukui, K.: Accounts. Chem. Res. **14**, 363 (1981)
17. Landau, L.: Phy. Z. Sowjetunion **2**, 46 (1932)
18. Zener, C.: Proc. Roy. Soc. Ser. **A137**, 696 (1932)
19. Nikitin, E. E., in: Chemische Elementarprozesse, p. 43, Hartmann, H., Ed. Berlin: Springer-Verlag 1968
20. Longuet-Higgins, H. C., Abrahamson, G. W.: J. Am. Chem. Soc. **87**, 2045 (1965)
21. Atkins, P. W.: Molecular Quantum Mechanics, second edition, p. 336. Oxford, New York: Oxford University Press 1983
22. Morihashi, K., Kikuchi, O., Suzuki, K.: Chem. Phys. Lett. **90**, 346 (1982)
23. Van der Lugt, W. Th. A. M., Oosterhoff, L. J.: J. Am. Chem. Soc. **91**, 6042 (1969)
24. Kikuchi, O.: Bull. Chem. Soc. Jpn. **47**, 1551 (1974)
25. Grimbert, D., Segal, G., Devaquet, A.: J. Am. Chem. Soc. **97**, 6629 (1975)
26. Hehre, W. J., Stewart, R. F., Pople, J. A.: J. Chem. Phys. **51**, 2657 (1969)
27. Hehre, W. J., Pople, J. A.: J. Am. Chem. Soc. **97**, 6941 (1975)